

Chapter 7

Co-Cr Alloys as Effective Metallic Biomaterials

Takayuki Narushima, Kyosuke Ueda, and Alfirano

Abstract Because of their excellent mechanical properties, high corrosion resistance, and high wear resistance, Co-Cr alloys have been recognized as effective metallic biomaterials and have been used as materials for dental and medical devices since a cast Co-Cr-Mo alloy, Vitallium, was developed in the 1930s. Further increases in the usage of Co-Cr alloys are still expected as well. In this chapter, first, the history and current status of biomedical Co-Cr alloys such as Co-28Cr-6Mo and Co-20Cr-15W-10Ni alloys are reviewed. Their microstructure, processing, and properties are then discussed. Control of the microstructure by optimization of chemical composition of the alloys and thermomechanical treatments is described, and newly developed processing techniques for grain refinement and newly found precipitates such as the π -phase and χ -phase are discussed. As a novel process for implant fabrication, an additive manufacturing technique using an electron beam and a laser beam is mentioned. Finally, the mechanical properties and corrosion and wear resistances of the alloys are presented, and the relationships between the microstructure and properties of the Co-Cr alloys are discussed.

Keywords Co-Cr-Mo alloy • Co-Cr-W-Ni alloy • Stacking fault energy • Microstructure • Precipitation • Additive manufacturing • Wear resistance

7.1 Introduction

Co-Cr alloys have been established as metallic biomaterials essential for orthopedic, cardiovascular, and dental fields because of their excellent mechanical properties, high corrosion resistance, and high wear resistance [1–3]. Their wear resistance

T. Narushima (✉) • K. Ueda
Department of Materials Processing, Tohoku University,
6-6-02 Aza Aoba, Aramaki, Aoba-ku, Sendai 980-8579, Japan
e-mail: narut@material.tohoku.ac.jp

Alfirano
Metallurgy Engineering Department, Sultan Ageng Tirtayasa University, Cilegon, Indonesia

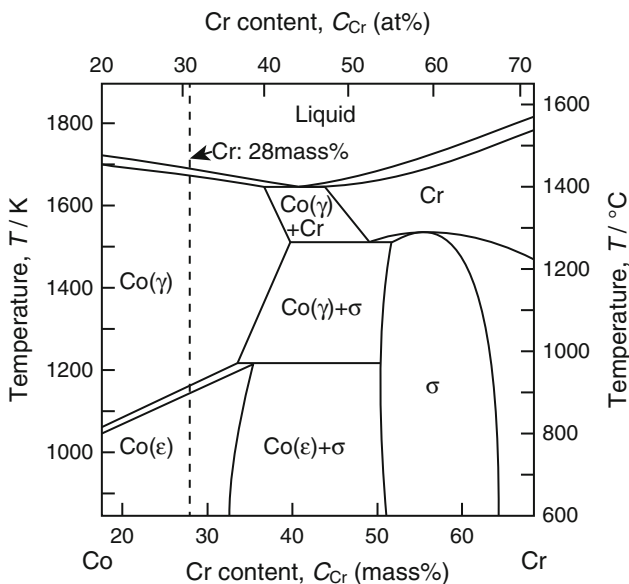
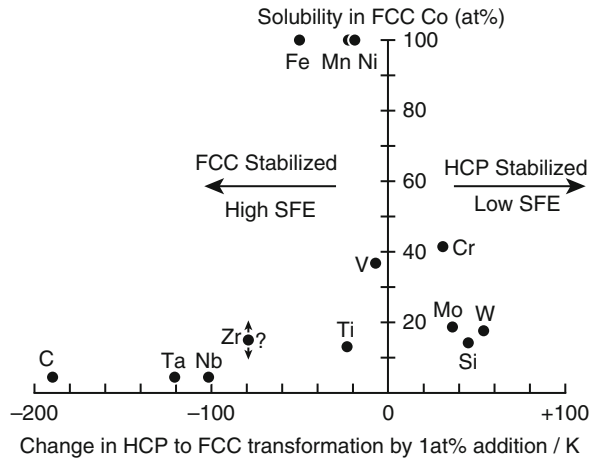


Fig. 7.1 Binary phase diagram of the Co-Cr system [6]

properties are particularly excellent as compared with those of other metallic biomaterials such as stainless steels and Ti alloys.

Pure Co undergoes an allotropic transformation at 690 K from the high-temperature γ -phase with the fcc (face-centered cubic) structure to the low-temperature ϵ -phase with the hcp (hexagonal close-packed) structure [4, 5]. This transformation is shear dominant with thermal hysteresis; therefore, it has been classified as martensitic [5]. The transformation temperature is changed by the addition of alloying elements to Co. In particular, biomedical Co-Cr alloys contain more than 20 mass% Cr, which improves the corrosion resistance by forming a passive layer consisting mainly of Cr oxide. The Co-Cr binary phase diagram is shown in Fig. 7.1 [6]. The addition of Cr increases the transformation temperature. The transformation temperatures in Co-20mass%Cr and Co-30mass%Cr alloys are around 1,100 and 1,200 K, respectively. Figure 7.2 summarizes the effects of alloying elements on the temperatures of the transformation from the hcp phase to the fcc phase of Co alloys [5]. The horizontal axis shows the change in the temperature of the hcp-to-fcc transformation from that for pure Co per 1at% of the alloying element, and the vertical axis shows the solubility of the alloying element in fcc Co. Alloying elements such as Fe, Mn, Ni, and carbon lower the hcp-to-fcc transformation temperature; they are fcc stabilizers. On the other hand, Mo, W, and Si increase the hcp-to-fcc transformation temperature and are hcp stabilizers, like Cr. This martensitic transformation is closely related to the microstructure and mechanical and chemical properties of the Co-Cr alloys.

Fig. 7.2 Effects of alloying elements on the temperature of the transformation from hcp Co to fcc Co as a function of solubility of the elements in fcc Co [5]



In this chapter, first, the history and current status of biomedical Co-Cr alloys such as Co-28mass%Cr-6mass%Mo and Co-20mass%Cr-15mass%W-10mass%Ni alloys are briefly reviewed. Their microstructure, processing, and properties are then discussed. Control of the microstructure of Co-Cr alloys is essential for practical applications, as it is for other metallic materials. Therefore, the effects of different processing techniques and the alloy composition including minor alloying elements on the microstructure are described with a focus on grain refinement and precipitation. As a novel processing technique for implant fabrication, an additive manufacturing technique using an electron beam and a laser beam is mentioned. Finally, the mechanical properties and corrosion and wear resistances of the alloys are presented. Hereafter, the chemical composition of the alloys is reported in units of mass%, although the mass% notation is omitted.

7.2 Co-Cr Alloys as Metallic Biomaterials

7.2.1 History

Co-based alloys in the Co-Cr and Co-Cr-W systems have been established since the early 1900s, and the Stellite alloys manufactured by Haynes became important industrial materials for wear-resistant hardfacing applications [5]. In the 1930s, a cast Co-Cr-Mo alloy, Vitallium, was developed, a technique for the lost-wax (investment) casting of the alloy was established, and the alloy was commercialized for dental prosthetics [7, 8]. Venable and Stuck used Vitallium devices for internal fixation of fractures and showed in the late 1930s that the alloy can be used in medical implants [9–11]. Vitallium was also used for prosthetic acetabular cups by Smith-Petersen in the late 1930s [12, 13]. These cups were used in the standard

method for hip reconstruction until total hip replacement operations were introduced in the 1960s [12]. In the 1950s and early 1960s, metal-on-metal-type and metal-on-polymer-type artificial hip joints using Vitallium were developed. The former are represented by the McKee-Farrar joint, and the latter were pioneered by Charnley [14]. Other Co-Cr alloys such as Co-Cr-W-Ni (L-605, HS25, ASTM F 90) [15], Co-Ni-Cr-Mo (MP35N, ASTM F 562), and Co-Cr-Fe-Ni-Mo (Elgiloy, ASTM F 1058 grade 1) system alloys, which are still used in practical applications at the present time, had been developed in the early 1960s. Thus, the Co-Cr alloys have a long history consisting of more than 80 years of use as dental and medical materials.

Currently, cast and wrought Co-Cr alloys are widely used for implants such as artificial joints, denture wires, and stents. Metal-on-metal-type total hip replacements made of Co-Cr-Mo alloys were revived in the late 1980s [14] because the loosening of the metal-on-UHMWPE (ultrahigh molecular weight polyethylene)-type artificial hip joints was found to be related to osteolysis caused by the formation of UHMWPE wear debris [16]. Recently, however, a decrease in the number of stemmed metal-on-metal-type artificial hip joints made of Co-Cr-Mo alloys used for hip replacements in England and Wales was reported [17].

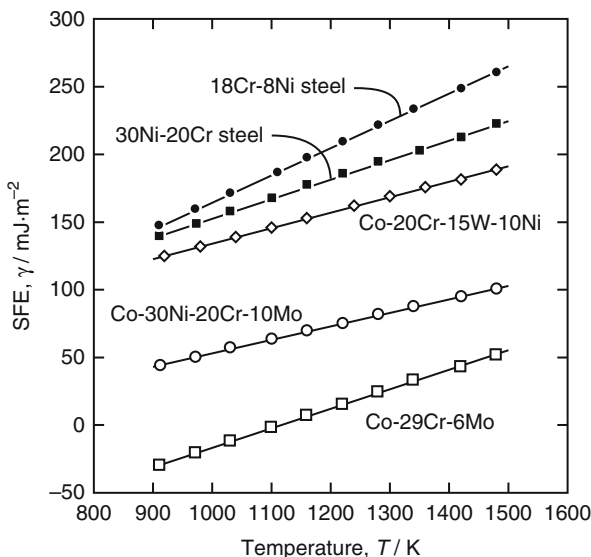
7.2.2 Types of Co-Cr Alloys

With their long history of practical applications, Co-Cr alloys have been listed in the ASTM standards for surgical implant applications [18]. Table 7.1 shows the chemical compositions from the standards. The contents of not only the main alloying elements such as Cr, W, and Mo but also minor alloying elements such as carbon and nitrogen are standardized. ASTM F 75 is for castings, and the others are for wrought products. The maximum carbon content in ASTM F 75 (Co-28Cr-6Mo) is 0.35 mass%. The low carbon content in ASTM F 75 alloy possibly causes the formation of the σ -phase (intermetallic compound, Co(CrMo)), which likely deteriorates the mechanical properties of the alloy. Carbon suppresses the formation of the σ -phase by forming carbides. The ASTM F 799 and F 1537 alloys, whose chemical compositions are registered as Co-28Cr-6Mo, have three types: Alloy 1 and Alloy 2 have low ($C \leq 0.14\text{mass}\%$) and high ($0.15\text{mass}\% \leq C \leq 0.35\text{mass}\%$) carbon contents, respectively, and Alloy 3 contains Al and La, which form oxide particles that provide dispersion strengthening [19].

Another classification of the Co-Cr alloys focuses on Ni content. The Ni content in ASTM F 75 alloy is required to be less than 0.5 mass%, and the Ni contents in ASTM F 799 and F 1537 alloys are required to be less than 1.0mass%. Other Co-Cr alloys such as ASTM F 90 (Co-20Cr-15W-10Ni), ASTM F 562 (Co-35Ni-20Cr-10Mo), and ASTM F 1058 (40Co-20Cr-16Fe-15Ni-7Mo) are allowed to contain Ni as an alloying element.

Figure 7.3 shows the stacking fault energies (SFEs) of three types Co-Cr alloys compared with those of Fe-based alloys [20]. The ASTM F 75 alloy, which is represented as Co-29Cr-6Mo in the figure, has a low SFE, so the hcp ϵ -phase with poor

Fig. 7.3 Temperature dependence of the calculated SFEs of Co-Cr alloys and Fe-based alloys [20]



workability would form during the cooling process in a casting or heat treatment. In contrast, Co-30Ni-20Cr-10Mo (close composition to ASTM F 562) and Co-20Cr-15W-10Ni (ASTM F 90) alloys, which contain Ni as an alloying element, exhibit mid-level and high SFEs, respectively. Therefore, the formation of the hcp ϵ -phase is suppressed, and these alloys have excellent hot and cold workability. In this context, Co-28Cr-6Mo alloys are basically unsuitable for wrought applications, but the workability in the Co-28Cr-6Mo alloys can be improved by optimizing the amounts of minor alloying elements such as nitrogen and by thermomechanical treatments (see Sect. 7.4.1).

7.2.3 Applications

Table 7.2 summarizes the applications of Co-Cr alloys. Cast Co-28Cr-6Mo (ASTM F 75) alloy has been used in the stem, ball, and cup of artificial hip joints including both metal-on-UHMWPE and metal-on-metal joints as well as in the sliding components of artificial knee joints. Since artificial knee joints have complicated shapes, investment casting is essential for their production. Wrought Co-28Cr-6Mo Alloy 1 and Alloy 2 (ASTM F 799 and F 1537) have been used in the joint replacements for hips, knees, shoulders, and so on. The Co-Cr alloys in the Co-Cr-W-Ni (ASTM F 90/F 1091), Co-Ni-Cr-Mo (ASTM F 562), and Co-Cr-Fe-Ni-Mo (ASTM F 1058) systems are used for wrought products that require a large deformation to fabricate. Since they exhibit excellent hot and cold workability and can be

Table 7.2 Applications of Co-Cr alloys

ASTM	Alloys (mass%)	Trade name	Application
F 75-12	Co-28Cr-6Mo	Vitalium (Howmedica, Inc)	Stem, ball, and cup of artificial joints
		Haynes-Stellite 21(HS21) (Cabot Corp.)	Fixation screws
		Protasul-2 (Sulzer AG)	Bone plates
		Zimaloy (Zimmer Inc.)	
F 799-11		BioDur CCM Plus Alloy (Carpenter Technology Corp.)	Joint replacements (hip, knee, shoulder)
F 1537-11			Fixation devices
F 90-09	Co-20Cr-15W-10Ni	Haynes-Stellite 25 (HS25) (Cabot Corp.)	Fixation wires
F 1091-12		L-605 (Carpenter Technology Corp.)	Vascular stents Heart valves
F 562-13	Co-35Ni-20Cr-10Mo	MP35N (SPS Technologies, Inc.)	Lead conductor wires
F 688-10		Biophase (Richards Medical Co.)	Springs
F 961-08		Protasul-10 (Sulzer AG)	Stylets Catheters Orthopedic cables Cardiovascular stents
F 1058-08	40Co-20Cr-16Fe-15Ni-7Mo	Elgiloy (Elgiloy Ltd.)	Arch wires
		Phynox (ArcelorMittal Stainless & Nickel Alloys) Conichrome (Carpenter Technology Corp.)	Springs Lead conductor wires Surgical clips Balloon-expandable stents (annealed) Self-expanding stents (aged)

strengthened by cold working, they have been used in fixation wires, vascular stents, springs, catheters, surgical clips, orthodontic dental archwires, and so on.

7.3 Microstructure and Processing in Co-Cr Alloys

7.3.1 Grain Refinement

Grain refinement can be used to strengthen metallic materials while maintaining their ductility. It is known that ultrafine grains smaller than 1 μm have been produced by severe plastic deformation; however, the severe plastic deformation techniques have not been applied to Co-Cr-Mo alloy parts because of their dual-phase microstructure and the strain-induced martensitic transformation during plastic deformation from the γ -phase to the ϵ -phase [21].

The grain refinement of Co-Cr-Mo alloys using conventional hot-compression deformation [21] and reverse transformation [22] has been reported. Yamanaka et al. [21] reported an ultrafine-grained microstructure with a grain size of around 0.6 μm obtained by the conventional hot-compression deformation of Co-29Cr-6Mo alloy with low carbon and low nitrogen contents. This microstructure was formed by dynamic recrystallization at 1,323 K under a strain rate of 0.1 s^{-1} from an initial average grain size of 40 μm . It was suggested that this fine microstructure was a product of the inhomogeneity in the local strain distribution induced by planar slips and deformation twins due to the lower SFE of this alloy at elevated temperatures [23]. A Co-29Cr-6Mo alloy with an average grain size of 0.8 μm produced by hot-compression deformation exhibited a significantly high 0.2 % proof strength of 1,330 MPa [24]. Kurosu et al. [22] developed a grain refinement process based on the reverse transformation from a lamellar (hcp ϵ -phase+Cr₂N) phase to an fcc γ -phase for the Co-27Cr-5Mo-0.16N alloy. Their process consisted of a two-step heat treatment without a hot or cold plastic transformation: solution-treated alloy was subjected to isothermal aging at 1,073 K for 90 ks to form a lamellar structure consisting of the hcp ϵ -phase+Cr₂N, and then the aged alloy with the complete lamellar microstructure was reverse-treated at a temperature of 1,273–1,473 K. The temperatures of 1,073 K and 1,273–1,473 K are in the stability regions for the ϵ -phase and γ -phase, respectively. The average grain size was reduced from 200 μm initially to 20–25 μm . Figure 7.4 shows the stress-strain curves of the Co-27Cr-5Mo-0.16N alloys after solution treatment (ST), aging treatment (AT), and reverse treatment (RT) at 1,273 K for 300 s [22]. The tensile strength was improved by the reverse transformation, while the ductility remained almost the same.

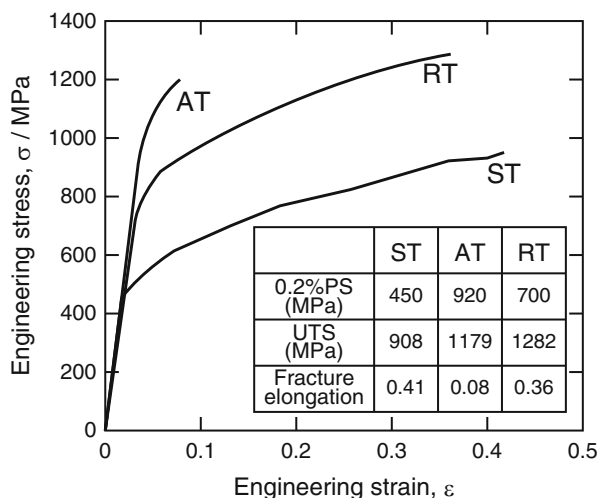


Fig. 7.4 Stress-strain curves of the Co-27Cr-5Mo-0.16N alloys after solution treatment (ST), aging treatment (AT), and reverse transformation (RT) at 1,273 K for 300 s. A table of the mechanical properties for each specimen is shown as an inset in the figure (Reprinted from Ref. [22], Copyright 2010, with permission from Elsevier)

7.3.2 Precipitation

Precipitates in the Co-Cr alloys are known to affect the mechanical properties [25, 26] and corrosion [27–29] and wear [30–34] resistances of both cast and wrought products. Therefore, knowledge of the precipitates present in as-cast alloys and after heat treatment is essential for establishing reasonable production processes for biomedical Co-Cr alloy devices.

The precipitates in Co-Cr alloys are classified into intermetallic compounds and carbonitrides [1]. Therefore, the carbon and nitrogen contents in Co-Cr alloys significantly affect the phase and morphology of the precipitates. Figure 7.5 shows the microstructures of as-cast Co-28Cr-6Mo alloys with carbon contents of 0 to 0.41 mass% and nitrogen contents of 0 to 0.24 mass% [35, 36]. A dendrite matrix and interdendritic and grain boundary precipitates were observed in the alloys, except in Fig. 7.5e. The amount of precipitates increased with the carbon content in the alloys. As shown in Fig. 7.5e, no precipitates were detected in the as-cast Co-28Cr-6Mo-0.20N alloy. In addition, no precipitates were formed in Co-28Cr-6Mo-0.20N and Co-28Cr-6Mo-0.25N alloys even after heat treatment at temperatures of 1,473–1,573 K for up to 43.2 ks, and the microstructure consisted of a single fcc γ -phase [36]. Thus, the formation of the σ -phase and the martensitic transformation from the γ -phase to the ϵ -phase can be suppressed by the addition of nitrogen to Co-28Cr-6Mo alloys without added carbon. Up to 0.25 mass% nitrogen is allowed in the ASTM F 75, F 799, and F 1537 standards.

The morphologies of precipitates found in Co-Cr-Mo alloys are summarized in Fig. 7.6 [1]: blocky-dense morphologies (σ -phase, χ -phase, η -phase (M_6X - $M_{12}X$ type), and $M_{23}X_6$ type), starlike-dense morphologies (π -phase), starlike morphologies with striped patterns ($M_{23}X_6$ type), starlike morphologies with complicated microstructures (including M_7X_3 type), and lamellar cellular colony morphologies

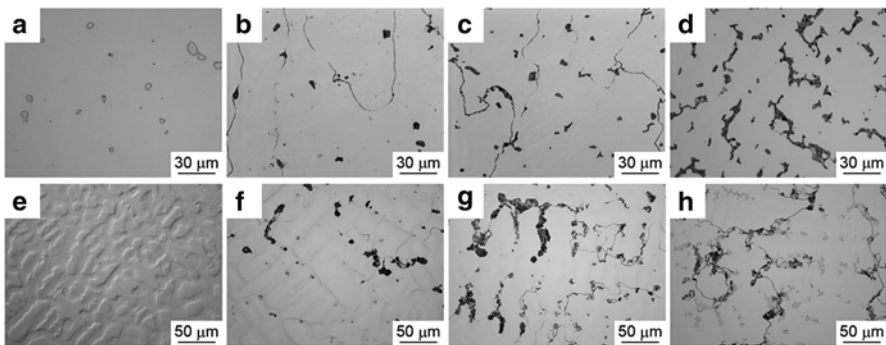


Fig. 7.5 Microstructures of as-cast Co-28Cr-6Mo alloys with various carbon and nitrogen contents: (a) 0C-0N, (b) 0.16C-0N, (c) 0.24C-0N, (d) 0.41C-0N, (e) 0C-0.2N, (f) 0.16C-0.2N, (g) 0.27C-0.24N, and (h) 0.34C-0.21N [35, 36]

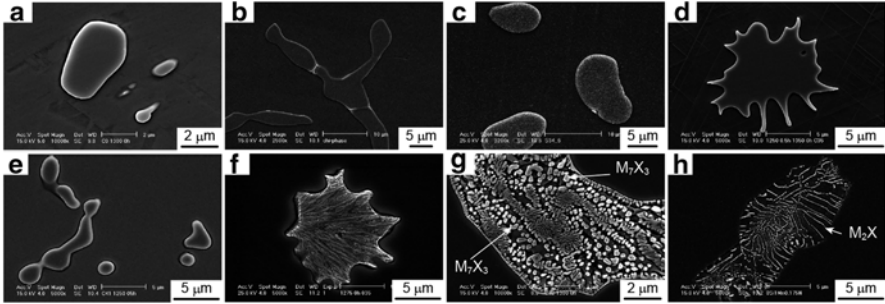


Fig. 7.6 Morphologies and phases of precipitates observed in biomedical Co-Cr-Mo alloys: (a) σ -phase (blocky dense), (b) χ -phase (blocky dense), (c) η -phase (blocky dense), (d) π -phase (starlike dense), (e) $M_{23}X_6$ type (blocky dense), (f) $M_{23}X_6$ type (starlike with stripe patterns), (g) M_7X_3 type (starlike with complicated microstructures), and (h) M_2X type (lamellar cellular colony) [1]

(M_2X type) have all been observed. In the notation for the precipitates, M refers to metallic elements such as Cr, and X refers to carbon and/or nitrogen. Clemow and Daniell [37] reported that the starlike shape was attributable to incipient melting around the edges of the carbide particles. The starlike shape of π -phase confirms that the π -phase forms under conditions where a liquid phase coexists. The $M_{23}X_6$ -type precipitate contains little nitrogen, i.e., it is almost carbide [1], and it is coherent with the γ -phase because its lattice constant is around 3 times of that of the γ -phase. The M_2X -type precipitate is a nitrogen-rich carbonitride that forms in nitrogen-containing Co-Cr-Mo alloys [1, 36, 38]. The η -phase [38] and π -phase [39] are carbon-rich carbonitrides, while the σ -phase [1] and χ -phase [1, 40] are intermetallic compounds. The formation of M_7X_3 -type precipitates in the Co-Cr-Mo alloys was suggested by Kilner et al. [41] and was confirmed by the present authors [39]. However, the chemical composition of the M_7X_3 -type precipitate has not been clarified, because its size was too small to be analyzed (see Fig. 7.6g). The alloying elements affect the stabilization of the precipitates: carbon stabilizes the $M_{23}X_6$ -type and M_7X_3 -type precipitates [39], nitrogen stabilizes the M_2X -type and η -phase precipitates, and Si stabilizes the η -phase [42] and χ -phase [1] precipitates. The $M_{23}X_6$ -type and η -phase precipitates were detected in Co-20Cr-15W-10Ni (ASTM F 90) alloy after heat treatment, although the as-forged alloy did not contain precipitates.

The presence of the π -phase [35, 39] and χ -phase [40, 43] was revealed by the present authors. Figure 7.7a shows the X-ray diffraction (XRD) pattern of precipitates electrolytically extracted from as-cast Co-28Cr-6Mo-0.16C-0.13N alloy [36]. The main reflections of the precipitate were in good agreement with the pattern of a $(Cr,Mo)_{12}(Fe,Ni)_{8-x}N_{4-z}$ -type nitride (JCPDS card no. 26-0428) that was detected as a precipitate after aging of an Fe-25Cr-28Ni-2Mo-0.31N alloy [44]. This nitride phase is referred to as the π -phase [45] and exhibits a β -Mn structure. Its chemical composition can be ideally represented as M_2T_3X , where M and T are metallic elements with low and high affinities for X (carbon and/or nitrogen),

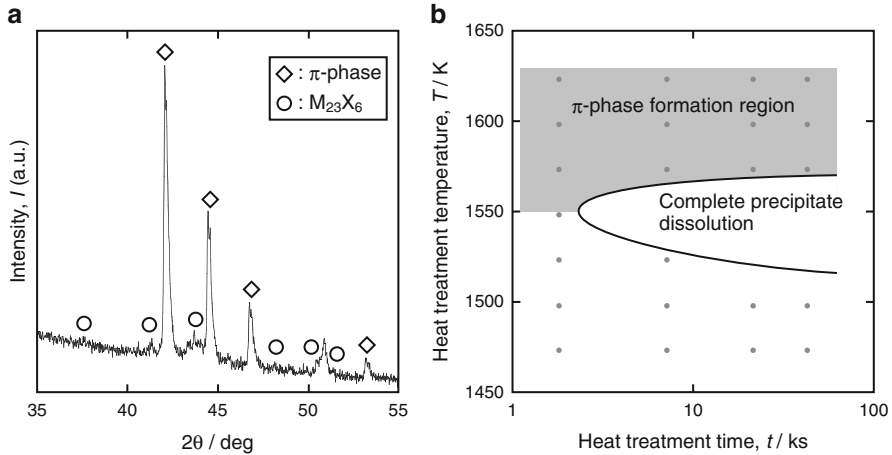


Fig. 7.7 (a) XRD pattern of precipitates electrolysically extracted from as-cast Co-28Cr-6Mo-0.16C-0.13N alloy and (b) schematic illustration of the formation region of the π -phase in Co-28Cr-6Mo alloys during heat treatment [36]

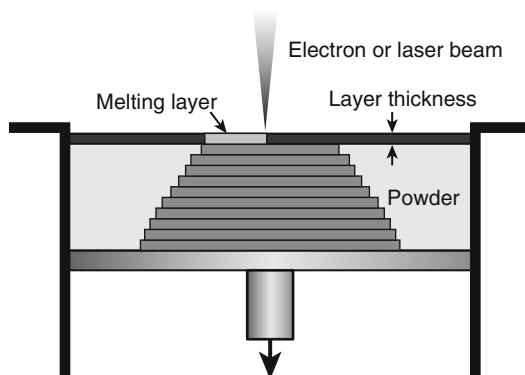
respectively. Figure 7.7b schematically shows the region where the π -phase was detected after heat treatment of the Co-28Cr-6Mo alloys. The formation of the π -phase is confirmed at temperatures of 1,548–1,623 K, where partial melting occurs in the alloys. The formation of the π -phase under the partial melting conditions was observed in the Co-28Cr-6Mo alloys from almost all of the carbon content region ($C \leq 0.35$ mass%) allowed by the ASTM F 75 standard. It was especially marked in the alloy with a carbon content of around 0.15mass%. Whether a π -phase precipitate is present in the alloys at room temperature depends on the cooling rate from the high temperatures at which the π -phase formed. Rapid cooling would be required to retain the π -phase precipitate in the alloys. A lower cooling rate seems to cause the π -phase to transform into other phases such as the $M_{23}X_6$ -type + metallic fcc γ -phase.

The χ -phase has an α -Mn structure with 58 metallic atoms in the unit cell [46, 47]. The presence of the χ -phase as a precipitate in Fe-based alloys after isothermal heat treatment was reported previously [48, 49]. The χ -phase precipitate is considered to be harmful in Fe-based alloys because it is deleterious to their mechanical properties. As for Co-Cr-Mo alloys, the heat treatment periods and chemical compositions for which the χ -phase is formed are limited. Therefore, it is relatively easy to prevent the formation of the χ -phase during the fabrication of Co-Cr-Mo alloy devices.

7.3.3 Novel Processing for Implant Fabrication

Recently, additive manufacturing for metals has been paid much attention as a process for producing complex three-dimensional structures from precursor powders [50]. This technique can be used to make orthopedic implants optimized for each

Fig. 7.8 Schematic diagram of additive manufacturing using electron beam melting and laser beam melting



patient's needs or skeletal structure. These custom-made implants are regarded as next-generation biomedical devices, and bone plates/screws, intramedullary nails, artificial joints, and so on are all expected to be fabricated using this technique [51]. Additive manufacturing using electron beam melting [52–54] and laser beam melting/sintering [55–58] has been performed to produce Co-Cr implants. In these techniques, CAD data for the implants are converted to data slices with heights of 20–100 μm . Using the slice data, an electron beam or a laser beam is irradiated onto a Co-Cr alloy powder with controlled particle size for melting and casting in a layer-by-layer manner (Fig. 7.8). Therefore, it is possible to precisely control the overall porosity and the size, shape, distribution, and direction of pores in the implants [59]. Electron beam melting is conducted under vacuum, while laser melting is operated under various atmospheres [60].

Gaytan et al. fabricated fully dense cylindrical and orthogonal structures and knee implant components by electron beam melting using Co-26Cr-6Mo-0.2C alloy powder [52, 53]. They observed Cr_{23}C_6 carbide arrays with dimensions of 2 μm in the building plane perpendicular to the building direction, which formed carbide columns in the vertical plane parallel to the building direction [52]. Hot isostatic pressing at 1,473 K produced an equiaxed fcc γ -phase grain structure with some grain boundary carbides. The anisotropy of the microstructures and mechanical properties of the as-cast Co-28Cr-6Mo-0.23C-0.17N alloy products fabricated by electron beam melting was also reported [54].

Selective laser melting has been applied to Co-Cr alloy implants in the dental [57, 58] and medical fields [55, 56]. Takaichi et al. [57] examined the microstructure, mechanical properties, and metal elution of the Co-29Cr-6Mo alloy products fabricated with different laser powers and scan spacings. Dense structures were obtained for input energies higher than 400 $\text{J}\cdot\text{mm}^{-3}$, whereas porous structures were formed for input energies lower than 150 $\text{J}\cdot\text{mm}^{-3}$. They observed a microstructure with fine cellular dendrites in elongated grains parallel to the building direction. Furthermore, the fcc γ -phase was dominant in the fabricated structures, and its preferential $\langle 001 \rangle$ orientation was found to be along the building direction. The

anisotropy of the mechanical properties due to the unique microstructure was also reported [57]. Finally, laser deposition of Co-Cr alloys was performed to add surface coatings for biomedical applications [61, 62].

7.4 Properties of Co-Cr Alloys

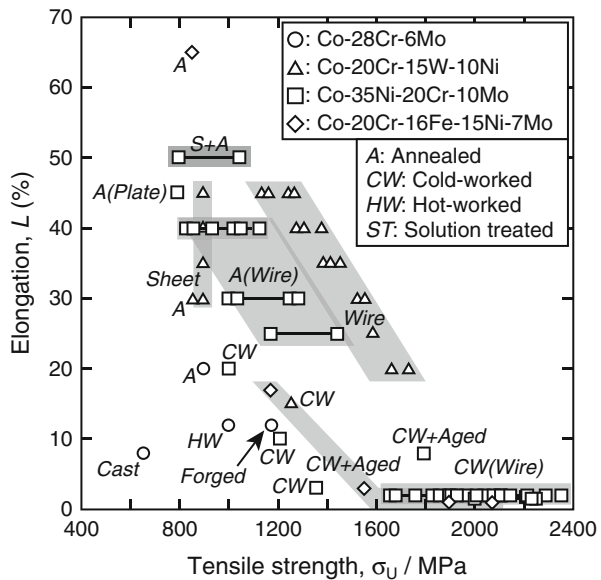
7.4.1 Mechanical Properties

Figure 7.9 summarizes the minimum requirements in the ASTM standards for the tensile strength and elongation of Co-Cr alloys. The mechanical strength and ductility of Co-Cr alloys can be changed over a wide range by controlling the microstructure using alloying and thermomechanical treatments, as is the case for other metallic materials.

The addition of small amount of alloying elements to cast Co-28Cr-6Mo (ASTM F 75) alloys is an effective way of controlling the microstructure. The addition of Zr [63] to ASTM F 75 alloys can yield a fine microstructure of the as-cast materials, resulting in increased tensile strength and elongation.

Nitrogen is an effective alloying element for improving the workability of wrought Co-28Cr-6Mo alloys [64], because it suppresses the σ -phase formation and γ -to- ϵ martensitic transformation, as described in Sect. 7.3.2. It has been reported that nitrogen stabilizes the γ -phase in the Co-29Cr-6Mo alloy by increasing the energy barrier for the γ -to- ϵ transformation and thus lowering the kinetic rate of the

Fig. 7.9 Tensile strength and elongation required for biomedical Co-Cr alloys in ASTM standards



transformation by forming Cr-N short-range order [65] or nanoscale Cr₂N precipitates in the γ matrix [66]. In fact, it has been reported that the addition of nitrogen improves the hot-working properties of the Co-28Cr-6Mo-0.16N alloy in the temperature range between 1,273 and 1,473 K [67]. The addition of nitrogen to Co-Cr-Mo alloys also increases their mechanical strength [68, 69]. It was reported [69] that strengthening of Co-29Cr-6Mo alloys was caused by the nanosized Cr₂N precipitates in the γ matrix. Better elongation and workability were achieved in the alloy with a nitrogen content of 0.10 mass%, where the γ -to- ϵ martensitic transformation was completely suppressed. However, the further addition of nitrogen was reported to slightly decrease the elongation to failure because of the enhanced formation of annealing twins [69].

Carbide precipitation was reported to increase the tensile strength but decrease the elongation and workability of Co-Cr-Mo alloys, although these properties depend on the size and distribution of the precipitates.

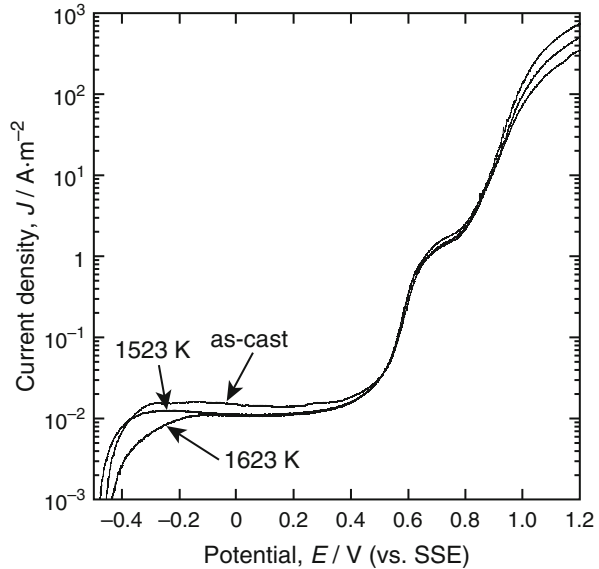
Recently, an increase in the Cr content up to 34 mass%, which is above the ASTM F 75 composition range, was reported to increase the nitrogen solubility in Co-Cr alloys and improve the mechanical strength and ductility under as-cast condition [70]. Finally, a nitrogen-containing Co-33Cr-6Mo alloy with excellent ductility was reported to be promising for fabricating dentures with adjustable clasps using one-piece casting [71].

7.4.2 Corrosion Resistance

The excellent corrosion resistance of Co-Cr alloys is caused by the passive layer on their surface, which prevents further corrosion under biological conditions. The passive layer formed on Co-Cr-Mo alloy after polishing in pure water consisted of complex oxides of Cr and Co with a small amount of Mo oxides including hydroxyl groups, and its thickness was 2.5 nm [72, 73]. It is known that passive layers in contact with electrolytes undergo a continuous process of partial dissolution and reprecipitation from the microscopic viewpoint. Co was dissolved from the passive layer during immersion in Hanks' solution and a cell culture medium and during incubation in a cell culture. In this way, a passive layer consisting of mainly Cr oxide with small amount of Mo oxide was reconstructed [73]. Hodgson et al. [74] investigated the passive layer of a Co-28Cr-Mo alloy in simulated biological solutions using X-ray photoelectron spectroscopy (XPS). They discovered that the major component dissolving from the alloy was Co and that the passive layer was mainly Cr(III) oxide along with a smaller amount of Cr(III) hydroxide.

Figure 7.10 shows the anodic polarization curves of as-cast and heat-treated Co-28Cr-6Mo-0.24C alloys in Hanks' solution. The heat treatment was conducted at 1,523 and 1,623 K for 43.2 ks. The alloy heat-treated at 1,523 K had no precipitates, while the main precipitates in the as-cast alloy and the alloy heat-treated at 1,623 K were of M₂₃X₆ type and π -phase, respectively. The effect of the precipitates on the corrosion resistance of the alloys was not strong. However, Bettini et al. [29]

Fig. 7.10 Anodic polarization curves in Hanks' solution for as-cast Co-28Cr-6Mo-0.24C alloy and for alloys heat treated at 1,523 and 1,623 K



suggested that $M_{23}X_6$ -type and M_6X -type precipitates affected the corrosion resistance of heat-treated Co-28Cr-6Mo-0.2C alloy on the basis of their microscopic surface observations after an electrochemical potential was applied. They observed that carbide boundaries were preferential sites for metal dissolution and that carbides with nonuniform compositions might exhibit different dissolution rates. Precise analyses of the microstructures of the precipitates and the chemical composition in the vicinity of the precipitates are required to understand the corrosion mechanisms of Co-Cr alloys under biological conditions.

7.4.3 Wear Resistance

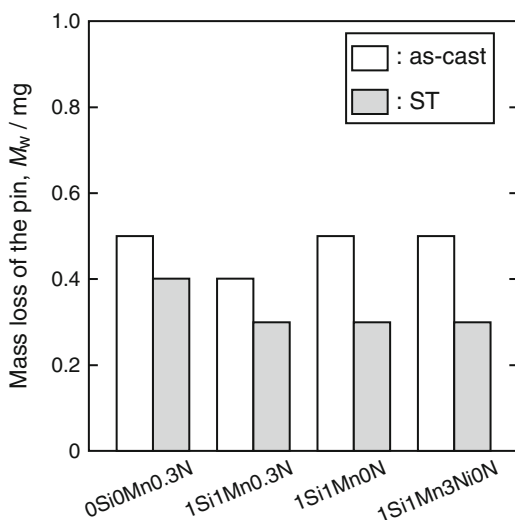
Excellent wear resistance is one of the characteristics of Co-Cr alloys. Such wear resistance is required in the sliding parts of artificial joints, for which Co-28Cr-6Mo (ASTM F 75, F 799, and F 1537) alloys are generally used. Therefore, the wear properties of the Co-28Cr-6Mo alloys are examined in this section.

As stated in Sect. 7.2.1, a decrease in the number of operations using stemmed metal-on-metal-type artificial hip joints made of Co-Cr-Mo alloys has been reported [17]. The main concerns regarding the use of metal-on-metal-type hip replacements are the formation of wear debris [75] and ion elution [76], which seem to be closely related to the microstructure of the Co-Cr-Mo alloy implants, which is influenced by the γ -to- ϵ phase transformation and precipitation of intermetallic compounds and carbonitrides.

Some studies have reported the effects of precipitation on the metal-on-metal wear behavior of Co-Cr-Mo alloys [32, 34, 77, 78]. Chiba et al. reported that marked abrasive wear was caused by precipitates such as σ -phase precipitates and that the Co-Cr-Mo alloys with ϵ -phase formed by strain-induced martensitic transformation during wear tests exhibited excellent wear resistance because of the increased hardness [34, 78]. Some studies have suggested that a high carbon content in Co-Cr-Mo alloys improves the wear properties [32, 77].

The present authors reported the pin-on-disk wear behavior in Kokubo solution for Co-Cr-Mo alloy pins with different precipitates and an Al_2O_3 disk [33]. As-cast and solution-treated (ST) Co-28Cr-6Mo-0.3N (0Si0Mn0.3N), Co-28Cr-6Mo-1Si-1Mn-0.3N (1Si1Mn0.3N), Co-28Cr-6Mo-1Si-1Mn (1Si1Mn0N), and Co-28Cr-6Mo-1Si-1Mn-3Ni (1Si1Mn3Ni0N) alloys were used as materials for the pins. The ST alloys had no precipitates, while the as-cast alloys contained π -phase, M_{23}X_6 -type, and M_2X -type precipitates, depending on the alloy composition. The mass loss of the pins after wear tests is shown in Fig. 7.11 [33]. The mass loss of the as-cast pins was higher than that of the ST pins. Figure 7.12 shows the surface morphologies of the as-cast and ST 1Si1Mn0.3N alloy pins after the wear tests [33]. The wear direction was from top to bottom in the figures. Continuous wear grooves were observed on the ST pin (Fig. 7.12b), while discontinuous deep wear grooves were detected in the as-cast pin after the wear tests (Fig. 7.12a). The formation of cavities and discontinuous deep grooves is likely to cause a higher mass loss for the as-cast pins than for the ST pins. Wear debris from both precipitates and the metallic matrix was found after wear tests of the as-cast pins. Some of the precipitates first detached from the metallic matrix, forming cavities during the wear tests, and then this debris caused discontinuous deep grooves through three-body abrasion.

Fig. 7.11 Mass loss of the pins after a wear test in Kokubo solution (Reprinted from Ref. [33], Copyright 2013, with permission from The Japan Institute of Metals and Materials)



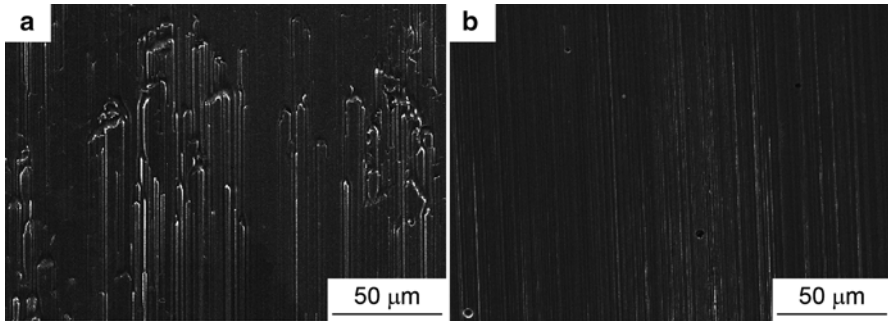


Fig. 7.12 SEM images of the surfaces of (a) as-cast and (b) ST pins of 1Si1Mn0.3N alloy after wear tests in Kokubo solution (Reprinted from Ref. [33], Copyright 2013, with permission from The Japan Institute of Metals and Materials)

The amounts of eluted ions of each metallic element (Co, Cr, Mo, Si, Mn, and Ni) after the wear tests are shown in Fig. 7.13 [33]. The Co/Cr and Co/Mn mass ratios for ions eluted from the 1Si1Mn3Ni0N alloy pin were calculated to be 53.1 and 225.0, which are much higher than the ratios of 2.1 and 49.3, respectively, calculated from the alloy composition. This means that the Cr and Mn ion contents are lower than expected based on the chemical composition of the alloy. EDX analysis suggested the formation of calcium phosphate on the wear tracks of the disks. The calcium phosphate included Cr and Mn, indicating that the Cr and Mn ions were preferentially incorporated into calcium phosphate [33].

Small amounts of Ni ions from Ni impurities in 0Si0Mn0.3N, 1Si1Mn0.3N, and 1Si1Mn0N alloy pins were detected after the wear tests. Decreasing the Ni content will be necessary to decrease Ni ion elution and thereby improve the safety of Co-Cr-Mo alloys.

7.5 Conclusions

The Co-Cr alloys have a long successful history of practical applications in the dental and medical fields since Vitallium was developed. It is impressive that Vitallium, or Co-Cr-Mo alloy, has been developed for dental applications and that the concept of Vitallium is still alive at the present time. The proportion of elderly people in the population is growing worldwide, and it is predicted that the number of patients suffering falls and deterioration of body functions will increase. Co-Cr alloys are seeing continued use in reconstruction devices for the human body, and the increases in their usage are expected. Co-Cr alloy has still much room for

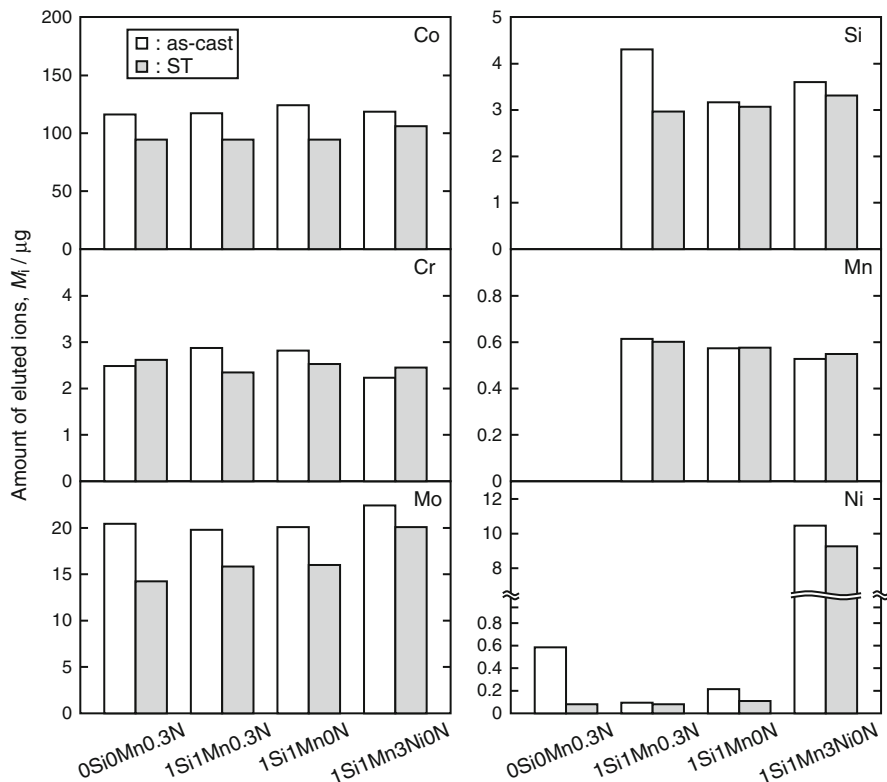


Fig. 7.13 Amounts of eluted Co, Cr, Mo, Si, Mn, and Ni ions after wear tests in Kokubo solution (Reprinted from Ref. [33], Copyright 2013, with permission from The Japan Institute of Metals and Materials)

improvement, and research into topics such as microstructure control using newly developed production processes and the optimization of alloy composition using metallic and light elements is required, especially for contents beyond the ASTM standards.

Acknowledgments This study was partially supported by a Grants-in-Aid for Scientific Research from the Ministry of Education, Culture, Sports, Science and Technology (MEXT), Japan.

References

1. Narushima T, Mineta S, Kurihara Y, Ueda K (2013) Precipitates in biomedical Co-Cr alloys. *JOM* 65:489–504
2. Narushima T (2010) New-generation metallic biomaterials. In: Niinomi M (ed) *Metals for biomedical devices*. Woodhead, Cambridge, pp 355–378

3. Niinomi M, Hanawa T, Narushima T (2005) Japanese research and development on metallic biomedical, dental, and healthcare materials. *JOM* 57(4):18–24
4. Davis JR (ed) (2000) *ASM specialty handbook: nickel, cobalt, and their alloys*. ASM International, Materials Park, p 356
5. Beltran AM (1987) Cobalt-base alloys. In: Sims CT, Stoloff NS, Hagel WC (eds) *Superalloys II*. Wiley, New York, pp 135–163
6. Baker H (ed) (1992) *ASM handbook, vol 3, Alloy phase diagrams*. ASM International, Materials Park, pp 2–140
7. Morral FR (1966) Cobalt alloys as implants in humans. *J Mater* 1:384–412
8. Morral FR (1968) The metallurgy of cobalt alloys – a 1968 review. *J Met* 20(7):52–59
9. Venable CS, Stuck WG, Beach A (1937) The effects on bone of the presence of metals; based upon electrolysis. *Ann Surg* 105:917–938
10. Venable CS, Stuck WG (1941) The use of Vitallium appliances in compound fractures. *Am J Surg* 51:757–778
11. Venable CS, Stuck WG (1943) Clinical uses of Vitallium. *Ann Surg* 117:772–782
12. <http://www.sciencemuseum.org.uk/broughttolife/objects/display.aspx?id=4899>
13. Smith-Petersen MN (1939) Arthroplasty of the hip: a new method. *J Bone Joint Surg* 21:269–288
14. Dowson D (2001) New joints for the millennium: wear control in total replacement hip joints. *Proc Inst Mech Eng* 215(Part H:JEIM):335–358
15. Wlodek ST (1963) Embrittlement of a Co-Cr-W (L-605) alloy. *Trans ASM* 56:287–303
16. Chan FW, Bobyn JD, Medley JB, Krygier JJ, Yue S, Tanzer M (1996) Engineering issues and wear performance of metal on metal hip implants. *Clin Orthop Relat Res* 333:96–107
17. Smith AJ, Dieppe P, Vernon K, Porter M, Blom AW (2012) Failure rates of stemmed metal-on-metal hip replacements: analysis of data from the National Joint Registry of England and Wales. *Lancet* 379:1199–1204
18. Mayer VA (ed) (2013) *Annual book of ASTM standards, section thirteen, medical devices and services, vol 13.01*. ASTM International, West Conshohocken
19. Wang KK, Berlin RM, Gustavson LJ (1999) A dispersion strengthened Co-Cr-Mo alloy for medical implants. In: Disegi JA, Kennedy RL, Pilliar R (eds) *Cobalt-based alloys for biomedical applications, ASTM STP 1365*. ASTM International, West Conshohocken, pp 89–97
20. Chiba A (2010) Co-Cr alloys. In: Hanawa T (ed) *Metals for medicine*. Japan Institute of Metals, Sendai, pp 84–92
21. Yamanaka K, Mori M, Kurosu S, Matsumoto H, Chiba A (2009) The grain refinement of biomedical Co-29Cr-6Mo alloy during conventional hot-compression deformation. *Metall Mater Trans A* 40A:1980–1994
22. Kurosu S, Matsumoto H, Chiba A (2010) Grain refinement of biomedical Co-27Cr-5Mo-0.16N alloy by reverse transformation. *Mater Lett* 64:49–52
23. Yamanaka K, Mori M, Chiba A (2012) Origin of significant grain refinement in Co-Cr-Mo alloys without severe plastic deformation. *Metall Mater Trans A* 43A:4875–4887
24. Yamanaka K, Mori M, Chiba A (2011) Mechanical properties of as-forged Ni-free Co-29Cr-6Mo alloys with ultrafine-grained microstructure. *Mater Sci Eng A* 528:5961–5966
25. Dobbs HS, Robertson JLM (1983) Heat treatment of cast Co-Cr-Mo for orthopaedic implant use. *J Mater Sci* 18:391–401
26. Gómez M, Mancha H, Salinas A, Rodríguez JL, Escobedo J, Castro M, Méndez M (1997) Relationship between microstructure and ductility of investment cast ASTM F-75 implant alloy. *J Biomed Mater Res* 34:157–163
27. Kuhn AT (1981) Corrosion of Co-Cr alloys in aqueous environments. *Biomaterials* 2:68–77
28. Yao MX, Wu JBC, Xu W, Liu R (2005) Metallographic study and wear resistance of a high-C wrought Co-based alloy Stellite 706K. *Mater Sci Eng A* 407:291–298
29. Bettini E, Eriksson T, Boström M, Leygraf C, Pan J (2011) Influence of metal carbides on dissolution behavior of biomedical CoCrMo alloy: SEM, TEM and AFM studies. *Electrochim Acta* 56:9413–9419

30. Wang A, Yue S, Bobyn JD, Chan FW, Medley JB (1999) Surface characterization of metal-on-metal hip implants tested in a hip simulator. *Wear* 225–229:708–715
31. Wimmer MA, Loos J, Nassutt R, Heitkemper M, Fischer A (2001) The acting wear mechanisms on metal-on-metal hip joint bearings: in vitro results. *Wear* 250:129–139
32. Varano R, Bobyn JD, Medley JB, Yue S (2006) The effect of microstructure on the wear of cobalt-based alloys used in metal-on-metal hip implant. *Proc Inst Mech Eng* 220(Part H: JEIM):145–159
33. Ueda K, Nakaie K, Namba S, Yoneda T, Ishimizu K, Narushima T (2013) Mass loss and ion elution of biomedical Co-Cr-Mo alloys during pin-on-disk wear tests. *Mater Trans* 54:1281–1287
34. Chen Y, Li Y, Kurosu S, Yamanaka K, Tang N, Koizumi Y, Chiba A (2014) Effects of sigma phase and carbide on the wear behavior of CoCrMo alloys in Hanks' solution. *Wear* 310:51–62
35. Mineta S, Namba S, Yoneda T, Ueda K, Narushima T (2010) Carbide formation and dissolution in biomedical Co-Cr-Mo alloys with different carbon contents during solution treatment. *Metall Mater Trans A* 41A:2129–2138
36. Mineta S, Alfirano Namba S, Yoneda T, Ueda K, Narushima T (2013) Phase and formation/dissolution of precipitates in biomedical Co-Cr-Mo alloys with nitrogen addition. *Metall Mater Trans A* 44A:494–503
37. Clemow AJT, Daniell BL (1979) Solution treatment behavior of Co-Cr-Mo alloy. *J Biomed Mater Res* 13:265–279
38. Alfirano Mineta S, Namba S, Yoneda T, Ueda K, Narushima T (2012) Precipitates in biomedical Co-Cr-Mo-C-N-Si-Mn alloys. *Metall Mater Trans A* 43A:2125–2132
39. Mineta S, Alfirano Namba S, Yoneda T, Ueda K, Narushima T (2012) Precipitates in biomedical Co-28Cr-6Mo-(0–0.41)C alloys heat-treated at 1473 K to 1623 K (1200 °C to 1350 °C). *Metall Mater Trans A* 43A:3351–3358
40. Narushima T, Mineta S, Alfirano Ueda K (2011) π -phase and χ -phase: new precipitates in biomedical Co-Cr-Mo alloys. In: Sasaki K (ed) *Interface oral health science 2011*. Springer, Berlin, pp 72–80
41. Kilner T, Pilliar RM, Weatherly GC, Allibert C (1982) Phase identification and incipient melting in a cast Co-Cr surgical implant alloy. *J Biomed Mater Res* 16:63–79
42. Alfirano Mineta S, Namba S, Yoneda T, Ueda K, Narushima T (2011) Precipitates in as-cast and heat-treated ASTM F75 Co-Cr-Mo-C alloys containing Si and/or Mn. *Metall Mater Trans A* 42A:1941–1949
43. Narushima T, Alfirano Mineta S, Namba S, Yoneda T, Ueda K (2011) Precipitates in biomedical Co-Cr-Mo-C-Si-Mn alloys. *Adv Mater Res* 277:51–58
44. Kikuchi M, Wakita S, Tanaka R (1973) β -manganese-type phase precipitated in high chromium-high nickel austenitic steels containing nitrogen. *Trans ISIJ* 13:226–228
45. Goldschmidt HJ (1957) Occurrence of the beta-manganese structure in transition metal alloys and some observations on chi-phase equilibria. *Metallurgia* 56:17–26
46. Kasper JS (1954) The ordering of atoms in the chi-phase of the iron-chromium-molybdenum system. *Acta Metall* 2:456–461
47. Joubert J-M, Phejar M (2009) Crystal chemistry and calphad modelling of the χ phase. *Prog Mater Sci* 54:945–980
48. Andrews KW (1949) A new intermetallic phase in alloy steels. *Nature* 164:1015
49. Redjaïmia A, Proult A, Donnadiou P, Morniroli JP (2004) Morphology, crystallography and defects of the intermetallic χ -phase precipitated in a duplex ($\delta + \gamma$) stainless steel. *J Mater Sci* 39:2371–2386
50. Harris ID (2012) Additive manufacturing: a transformational advanced manufacturing technology. *Adv Mater Process* 170:25–29
51. Okazaki Y (2012) Development trends of custom-made orthopedic implants. *J Artif Organ* 15:20–25

52. Gaytan SM, Murr LE, Martinez E, Martinez JL, Machado BI, Ramirez DA, Medina F, Collins S, Wicker RB (2010) Comparison of microstructures and mechanical properties for solid and mesh cobalt-base alloy prototypes fabricated by electron beam melting. *Metall Mater Trans A* 41A:3216–3227
53. Gaytan SM, Murr LE, Ramirez DA, Machado BI, Martinez E, Hernandez DH, Martinez JL, Medina F, Wicker RB (2011) A TEM study of cobalt-base alloy prototypes fabricated by EBM. *Mater Sci Appl* 2:355–363
54. Sun S-H, Koizumi Y, Kurosu S, Li Y-P, Matsumoto H, Chiba A (2014) Build direction dependence of microstructure and high-temperature tensile property of Co–Cr–Mo alloy fabricated by electron beam melting. *Acta Mater* 64:154–168
55. Vandenbroucke B, Kruth J-P (2007) Selective laser melting of biocompatible metals for rapid manufacturing of medical parts. *Rapid Prototype J* 13:196–203
56. Hunt JA, Callaghan JT, Sutcliffe CJ, Morgan RH, Halford B, Black RA (2005) The design and production of Co–Cr alloy implants with controlled surface topography by CAD–CAM method and their effects on osseointegration. *Biomaterials* 26:5890–5897
57. Takaichi A, Suyalatu NT, Joko N, Nomura N, Tsutsumi Y, Migita S, Doi H, Kurosu S, Chiba A, Wakabayashi N, Igarashi Y, Hanawa T (2013) Microstructures and mechanical properties of Co–29Cr–6Mo alloy fabricated by selective laser melting process for dental applications. *J Mech Behav Biomed Mater* 21:67–76
58. Al Jabbari YS, Koutsoukis T, Barmpagadaki X, Zinelis S (2014) Metallurgical and interfacial characterization of PFM Co–Cr dental alloys fabricated via casting, milling or selective laser melting. *Dent Mater* 30:e79–e88
59. Ryan G, Pandit A, Apatsidis DP (2006) Fabrication methods of porous metals for use in orthopaedic applications. *Biomaterials* 27:2651–2670
60. Momose W (2013) Advantages of electron beam melting technology and application as real mass-production. *Titan Jpn* 61:198–199
61. Meacock CG, Vilar R (2009) Structure and properties of a biomedical Co–Cr–Mo alloy produced by laser powder microdeposition. *J Laser Appl* 21:88–95
62. Wilson JM, Jones N, Jin L, Shin YC (2013) Laser deposited coatings of Co–Cr–Mo onto Ti–6Al–4V and SS316L substrates for biomedical applications. *J Biomed Mater Res B Appl Biomater* 101B:1124–1132
63. Lee S-H, Uchikanezaki T, Nomura N, Nakamura M, Chiba A (2007) Effects of zirconium addition on microstructures and mechanical properties of Co–29Cr–6Mo Alloy. *Mater Trans* 48:1084–1088
64. Mori M, Yamanaka K, Matsumoto H, Chiba A (2010) Evolution of cold-rolled microstructures of biomedical Co–Cr–Mo alloys with and without N doping. *Mater Sci Eng A* 528:614–621
65. Li YP, Yu JS, Kurosu S, Koizumi Y, Matsumoto H, Chiba A (2012) Role of nitrogen addition in stabilizing the γ phase of biomedical Co–29Cr–6Mo alloy. *Mater Chem Phys* 133:29–32
66. Yamanaka K, Mori M, Chiba A (2013) Nanoarchitected Co–Cr–Mo orthopedic implant alloys: nitrogen-enhanced nanostructural evolution and its effect on phase stability. *Acta Biomater* 9:6259–6267
67. Chiba A, Lee S-H, Matsumoto H, Nakamura M (2009) Construction of processing map for biomedical Co–28Cr–6Mo–0.16N alloy by studying its hot deformation behavior using compression tests. *Mater Sci Eng A* 513–514:286–293
68. Dempsey AJ, Pilliar RM, Weatherly GC, Kilner T (1987) The effects of nitrogen additions to a cobalt–chromium surgical implant alloy. Part 2 mechanical properties. *J Mater Sci* 22:575–581
69. Yamanaka K, Mori M, Chiba A (2014) Effects of nitrogen addition on microstructure and mechanical behavior of biomedical Co–Cr–Mo alloys. *J Mech Behav Biomed Mater* 29:417–426
70. Lee S-H, Nomura N, Chiba A (2008) Significant improvement in mechanical properties of biomedical Co–Cr–Mo alloys with combination of N addition and Cr-enrichment. *Mater Trans* 49:260–264

71. Yoda K, Suyalatu TA, Nomura N, Tsutsumi Y, Doi H, Kurosu S, Chiba A, Igarashi Y, Hanawa T (2012) Effects of chromium and nitrogen content on the microstructures and mechanical properties of as-cast Co–Cr–Mo alloys for dental applications. *Acta Biomater* 8:2856–2862
72. Smith DC, Pilliar RM, Metson JB, McIntyre NS (1991) Dental implant materials. II. preparative procedures and surface spectroscopic studies. *J Biomed Mater Res* 25:1069–1084
73. Hanawa T, Hiromoto S, Asami K (2001) Characterization of the surface oxide film of a Co–Cr–Mo alloy after being located in quasi-biological environments using XPS. *Appl Surf Sci* 183:68–75
74. Hodgson AWE, Kurz S, Virtanen S, Fervel V, Olsson C-OA, Mischler S (2004) Passive and transpassive behaviour of CoCrMo in simulated biological solutions. *Electrochim Acta* 49:2167–2178
75. Hallab NJ (2009) A review of the biologic effects of spine implant debris: fact from fiction. *SAS J* 3:143–160
76. Sargeant A, Goswami T (2007) Hip implants – Paper VI – ion concentrations. *Mater Des* 28:155–171
77. Tipper JL, Firkins PJ, Ingham E, Fisher J, Stone MH, Farrar R (1999) Quantitative analysis of the wear and wear debris from low and high carbon content cobalt chrome alloys used in metal on metal total hip replacements. *J Mater Sci Mater Med* 10:353–362
78. Chiba A, Kumagai K, Nomura N, Miyakawa S (2007) Pin-on-disk wear behavior in a like-on-like configuration in a biological environment of high carbon cast and low carbon forged Co–29Cr–6Mo alloys. *Acta Mater* 55:1309–1318